A landslide granular phase transition

Rory T. Cerbus[1,*], *Thierry* Faug[2,**], and *Hamid* Kellay[1,***]

[1]Laboratoire Ondes et Matiére d'Aquitaine (LOMA), 351 cours de la libération, 33405 Talence, France
[2]University Grenoble-Alpes, INRAE, UR ETNA, 2 rue de la Papeterie BP 76, F-38402 St-Martin-d'Hères, France

Abstract. Landslides appear in many different forms and sizes, from devastating debris flows to overly optimistic sand castles. A familiar and well-documented feature of all landslides is the positive correlation between volume and landslide runout. Larger landslides have a greater potential to reach farther. Here we explore the low volume limit and find a surprising negative correlation between volume and landslide runout. A decrease in volume leads to an increase in runout. In a series of experiments we systematically vary the landslide volume to reveal a transition between these two regimes.

1 Introduction

As Albert Heim observed as early as 1932 [1], landslides can sometimes travel many times further than would be naively predicted from an energy balance between the initial gravitational potential energy and dissipation by sliding friction. These long runouts are the source of much destruction, and thus have naturally become a focus of experimental, numerical, and theoretical inquiry. Different mechanisms have been proposed to explain the apparent decrease in (effective) friction [2–4], while others claim that this is simply the expected result of volumetric spreading [5]. Regardless, all evidence suggests that long runouts only occur in the limit of large landslide volumes.

Whether it be debris, rocks, or snow, the similarity between these geophysical flows and the flow of sand has led to the practice of laboratory experiments with flows of sand or glass beads being used as analogs of much larger geophysical flows such as landslides. In this spirit we conduct a series of simple experiments with nearly spherical glass beads which we release on an inclined glass plate to finally runout onto a flat glass plate. Surprisingly, in addition observing the classical decrease in effective friction at large volumes, we also observe decreased effective friction in the opposite limit of small landslide volumes. We relate this decrease in effective friction with a transition between a (granular) liquid and gas state, in which a change in particle density substantially affects the rheology of the flow.

2 Experimental procedure

2.1 Main experimental setup

As shown in the schematic in Fig. 1, our experimental setup is a simple geometry consisting of a flat glass plate inclined at an angle θ, connected with a level flat glass plate at a junction we define as $x = 0$. The results reported here are for $\theta \simeq 35°$. The inclined flat plate is 80 cm along its length and 65 cm wide. The level plate is made of two plates with the same dimensions but oriented so that the combined length in the runout direction is 130 cm and the width is 80 cm. The small junction between the two level plates is covered with transparent Scotch tape to minimize its effect on the landslide runout. The grains of average diameter $\langle d \rangle$ are initially placed in a rectangular plexiglass box resting a distance along the incline of $L_0 = 42.5$ cm from the junction between the inclined and level plates. The box has a horizontal width of 15 cm. The grains are released by rapidly raising the front metal sluice gate. The glass plates and grains are illuminated from be-

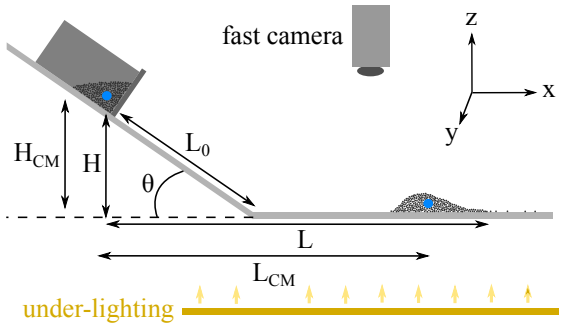

Figure 1. Schematic of experimental setup. The grains are released from a rectangular box by a sliding sluice gate at the front. The released grains slide down a flat glass plate inclined at an angle θ and eventually come to rest on a level flat glass plate. The motion and final position of the grains are observed with a fast camera. By illuminating the grains from below and calibrating the transmission intensity, the height distribution and thus center of mass can be accurately determined. The large (blue) dot indicates the initial and final center of mass positions with a difference in height given by H_{CM}, a difference in horizontal distance given by L_{CM}. The difference in height and horizontal position for the front position is given by H and L respectively.

*e-mail: rory.cerbus@u-bordeaux.fr
**e-mail: thierry.faug@inrae.fr
***e-mail: hamid.kellay@u-bordeaux.fr
A video is available at https://doi.org/10.48448/9wzj-5n94

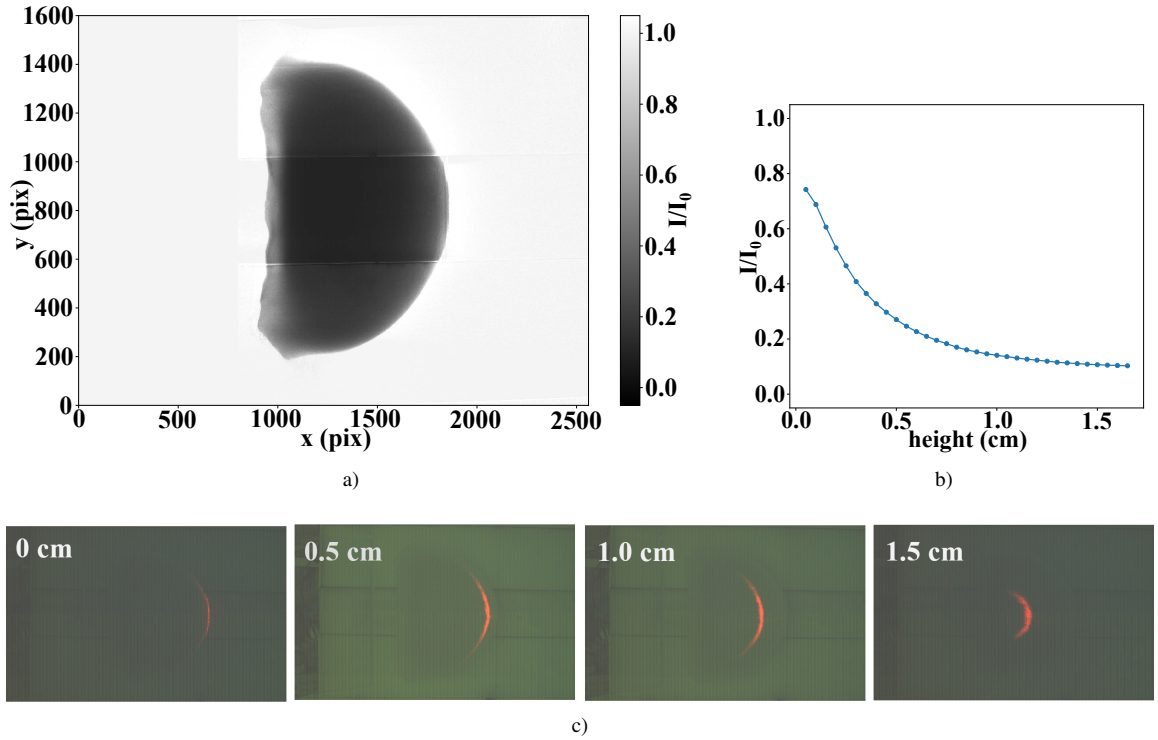

Figure 2. a) Normalized intensity image I/I_0 of a landslide. b) The resulting normalized intensity I/I_0 vs. height h calibration curve used to determine the height as a function of space $h(x, y)$. c) Images showing the laser sheet height positions used for the calibration.

low by several large LED panels which are powered by a stable DC voltage supply to ensure no light intensity variations in time. The grain positions and motion is observed with an overhead fast camera (Phantom) typically capturing at a frame rate of 100 Hz. The images are processed in a personal computer with programs written in Python using the standard image processing library OpenCV [6].

The key observables are the initial landslide height and the runout distance. Because a landslide is an extended body with nontrivial geometry, there are many ways to characterize height and distance. We focus on two features: the front position and the center of mass position. The initial height of the landslide front is $H = L_0 \sin\theta$, and the distance L is the horizontal distance between the initial front and the final front. Because of symmetry we focus attention at $y = 0$, the center, which is also the horizontal location of the grains which travel the farthest. While the initial front is well-defined, the final front can be disperse. We choose to identify the front as the furthest position where there is still a continuous (touching) monolayer of grains connected to the main landslide body. The initial center of mass position $(x_{\mathrm{CM},i}, y_{\mathrm{CM},i} = 0, z_{\mathrm{CM},i})$ is determined geometrically by measuring the grain pile dimensions with a ruler and assuming a uniform packing fraction after the particles are sprinkled into the box. In order to determine the center of mass of the final grain pile, which has a nontrivial geometry that differs for each initial volume, we use a novel optical technique.

Simply put, our optical technique maps the transmitted light intensity from the (underneath) LED lighting I, to height, h. First, we measure the background intensity $I_0(x, y)$ as a function of space (x,y). Then, with a large volume landslide, we measure the transmitted intensity field $I(x, y)$, also as a function of space. Although the lighting is uniform, by normalizing $I(x, y)$ with $I_0(x, y)$ we reduce any spatial non-uniformity even further (see Fig. 2a). Then, without moving the camera or landslide, we mount a laser light sheet on a translation stage and capture images of the landslide. From these images we can easily identify the locations where the laser light sheet intersects the grain pile for a large range of heights (see Fig. 2c). We thus calibrate the intensity by determining the normalized intensity I/I_0 as a function of height h (see Fig. 2b). Near $h \approx 0$ this calibration method suffers from the fact that there are few to no grains to illuminate, thus in practice we linearly extrapolate our calibration from the minimum reliable h in the calibration to $h = 0$. Using a linear extrapolation or simply disregarding any data outside of the calibration leads to nearly indistinguishable results. For this procedure we made the simplifying assumption that the transmissivity of the grain pile depends only on the height. We found that the estimated location of the center of mass is not sensitive to the calibration, so that even weighting with transmitted intensity instead of the calibrated height hardly changes the result. From this we determine the height map $h(x, y)$ and thus the final center of mass height $z_{\mathrm{CM},f} = \langle h \rangle = A^{-1} \int_0^\infty \int_0^\infty \hat{x} h(x, y) dx dy$, and final runout distance $x_{\mathrm{CM},f} = (A\langle h \rangle)^{-1} \int_0^\infty \int_0^\infty \hat{x} h(x, y) dx dy$, where A is the area for which $h(x, y)$ is nonzero. (We find that $y_{\mathrm{CM},f} \simeq y_{\mathrm{CM},i} = 0$.) In the integrals (sums), $h(x, y)$ is undefined outside of the grain pile. Thus the center of mass height is $H_{\mathrm{CM}} = z_{\mathrm{CM},i} - z_{\mathrm{CM},f}$, and the distance is $L_{\mathrm{CM}} = x_{\mathrm{CM},f} - x_{\mathrm{CM},i}$.

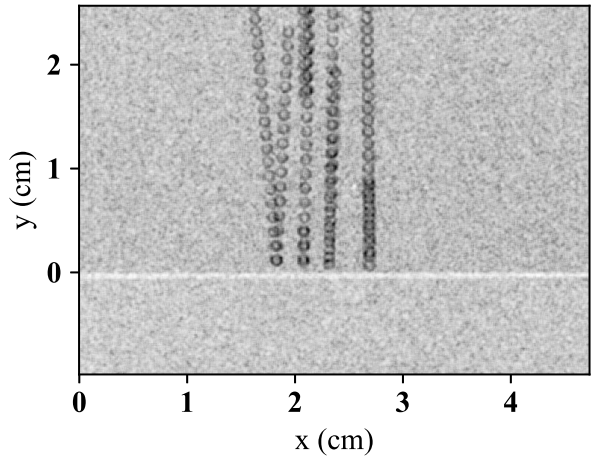

Figure 3. Example of images (strobed) used to track the particles and estimate velocity, size and shape for determining the mechanical properties. Grain velocities in these ancillary experiments ranged from $\sim$ 20cm/s to $\sim$ 140cm/s. When estimating the diameter and eccentricity, the glass bar, the edge of which is at $y = 0$ in the image, is removed. The particles used here are $\langle d \rangle \simeq 1$mm.

2.2 Mechanical properties

In addition, we developed a novel procedure to measure important mechanical properties of the grains, which are necessary to estimate important quantities such as dissipation. We sprinkle the grains in between two vertical glass plates and observe them with the same steady illumination and fast camera described in the main experimental setup (Sec. 2.1). In this way the particles generally do not touch and we can estimate their size and shape accurately. We fit an ellipse to each grain and defined the diameter of each grain as the average between the semi-major (a) and semi-minor (b) axes. The eccentricity is then ecc. $= \sqrt{1 - b^2/a^2}$, where 0 indicates a circle and 1 a line. To determine the coefficient of restitution e, we inserted a smooth glass bar in between the glass plates and tracked the grain motion before and after collision with the glass bar. Then $e = -v_f/v_i$, where v_i is the initial vertical velocity component and v_f is the final vertical velocity component. A coefficient of restitution $e = 1$ corresponds to a perfectly elastic collision. We used our own Python programs that utilise the OpenCV library [6] to process the images to determine the diameter and eccentricity, while we used the Trackpy package [7] to estimate the velocities to determine the coefficient of restitution. See Fig. 4 for a summary of the empirically-determined probability distributions of these mechanical properties.

3 Results

We performed a large set of experiments systematically varying the volume (mass) of the initial pile. Then we adopt the measures of runout most commonly used in the literature where the initial height is divided by the final horizontal distance. With our two measures of vertical and horizontal distance, we thus have two measures of runout: $\mu_{\rm CM} = H_{\rm CM}/L_{\rm CM}$ and $\mu_{\rm front} = H/L$. The reason for this symbol and this representation of the runout is that if the landslide were composed of a single block of glass unable to roll, then $\mu_{\rm front} \simeq \mu_{\rm CM} = \mu_{\rm glass}$, the dynamic coefficient of sliding friction between glass and glass. Thus any departures of $\mu_{\rm CM}$ and $\mu_{\rm front}$ from $\mu_{\rm glass}$ is a manifestation of the landslide's granular nature.

Fig. 5 shows the resulting $\mu_{\rm CM}$ and $\mu_{\rm front}$ vs. initial volume ($\langle d \rangle \simeq 508\mu$m). At low volumes the two measures of effective friction are similar as the center of mass and front positions hardly differ for small grain piles. As the initial volume increases, however, the two curves begin to deviate. The most prominent feature, shared by both curves, is their non-monotonic behavior with respect to initial volume. At low initial volumes both $\mu_{\rm CM}$ and $\mu_{\rm front}$ are increasing functions of volume. At a critical volume, apparently different for the two curves, they reach a maximum and begin to monotonically decrease thereafter. To our knowledge, this observation of non-monotonic effective friction with respect to initial volume is novel.

To uncover a mechanism for this non-monotonicity in the effective friction, we look to instantaneous images of the normalized landslide intensity (see the images on the right of Fig. 5). These reveal that the grain piles start out gaseous in appearance at low volumes but become increasingly dense as the volume is increased, suggestive of a granular gas-liquid phase transition. While a complete theory of granular gas-liquid phase transition is still lacking [8], several salient features of the two regimes are useful for a qualitative understanding of Fig. 5. In granular kinetic theory, the dissipation rate per unit volume is given by [8]: $\Gamma = \rho(1 - e^2) f(\phi) T^{3/2}/d$, where $f(\phi)$ is an increasing function of the packing fraction ϕ, ρ is the grain density, and T is the granular temperature. All else held constant, it stands to reason that ϕ is an increasing function of volume (at least at low volumes) and thus Γ is an increasing function of the initial volume, leading to an increase of effective friction at low volumes in the gaseous regime. In the dense regime, on the other hand, ϕ is large and varies little. Granular kinetic theory, at least in the form for which the Γ defined above is relevant, is no longer valid. The rheology in the dense flow regime is qualitatively different, with prominent theories such as the $\mu(I)$ rheology perhaps being more relevant. For this dense liquid regime, the decrease in $\mu_{\rm front}$ can perhaps partially be explained as a volumetric effect: a large volume landslide will spread out in all directions relative to its center of mass location more than a small volume landslide [5], although the slight decrease in $\mu_{\rm CM}$ suggests that more may be at play.

4 Conclusion

In summary, using a simple experimemtal setup we have observed a novel non-monotonic relationship between two measures of effective friction, $\mu_{\rm front}$ and $\mu_{\rm CM}$, with respect to initial landslide volume. We have provided preliminary evidence for an explanation that this non-monotonicity is a manifestation of a granular gas-liquid phase transition. Further experiments, including DEM simulations, are required to substantiate these claims.

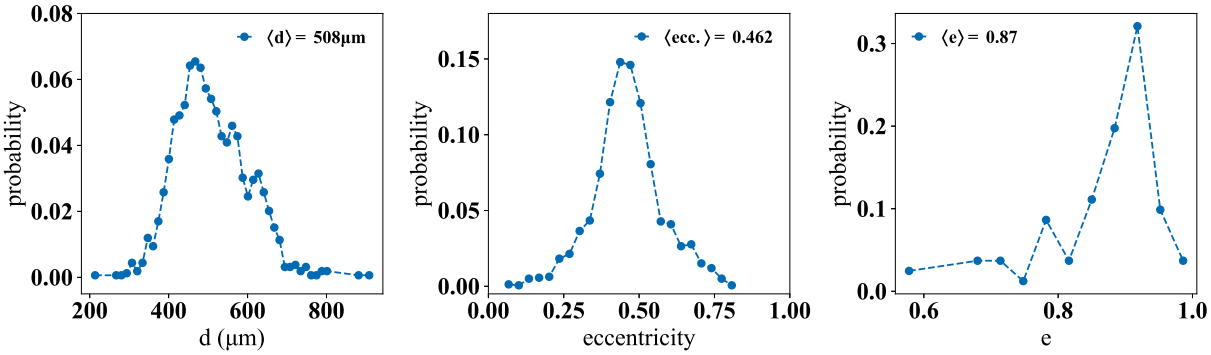

Figure 4. Left: Probability distribution of the grain sizes for the experiments reported here. Center: Probability distribution of the eccentricity (a measure of the deviation from a circle) for the grains. Right: Probability distribution of the coefficient of restitution of the grains. The distributions of d and ecc. can be well approximated by a gaussian distribution.

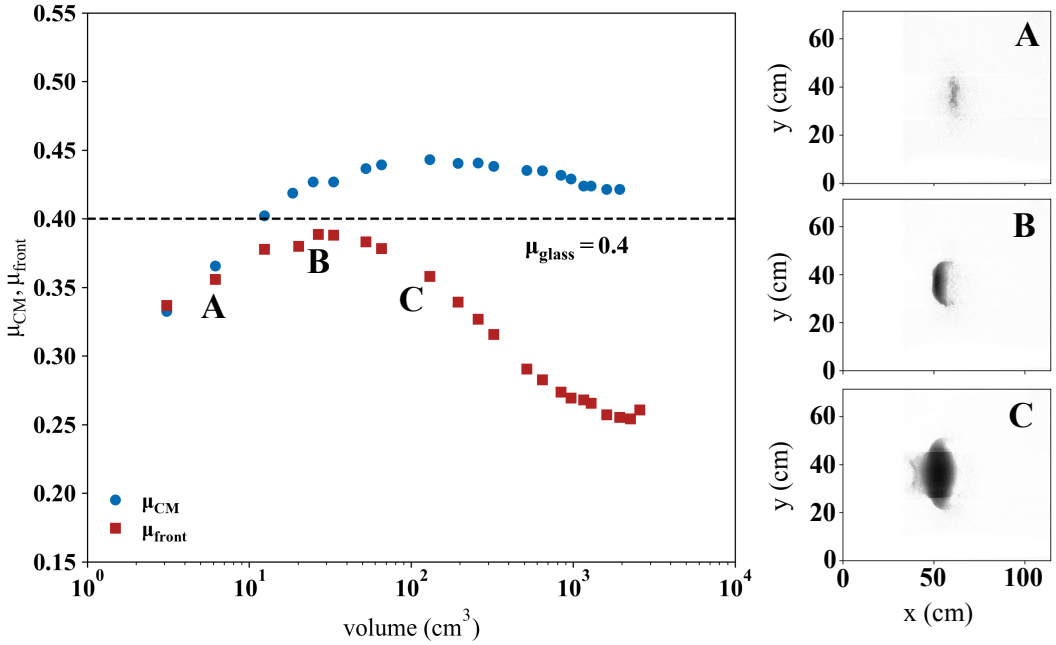

Figure 5. Left: Effective friction $\mu_{\mathrm{CM}} = H_{\mathrm{CM}}/L_{\mathrm{CM}}$ and $\mu_{\mathrm{front}} = H/L$ vs. initial volume. Right: Intensity (normalized) images during landslide motion $t = 0.5$s after the junction is first reached, with A, B and C corresponding to the data with the same notation on the left. As the initial volume increases, the landslides become more dense and less gaseous in appearance. This change in appearance corresponds with the non-monotonic behavior of the effective friction μ_{front} and μ_{CM}.

R.T.C. gratefully acknowledges the support of a Marie Skłodowska-Curie Action Individual Fellowship (MSCAIF).

References

[1] A. Heim, *Bergsturz und menschenleben*, 20 (Fretz & Wasmuth, 1932)
[2] B.C. Johnson, C.S. Campbell, H.J. Melosh, J. Geophys. Res. Earth Surface **121**, 881 (2016)
[3] R.M. Iverson, R.G. LaHusen, Sci. **246**, 796 (1989)
[4] T.R. Davies, Rock Mech. **15**, 9 (1982)
[5] S. Parez, E. Aharonov, Front. Phys. **3**, 80 (2015)
[6] G. Bradski, Dr Dobb's J. Softw. Tools **25**, 120 (2000)
[7] J.C. Crocker, D.G. Grier, J. Colloid Interface Sci. **179**, 298 (1996)
[8] B. Andreotti, Y. Forterre, O. Pouliquen, *Granular media: between fluid and solid* (Cambridge University Press, 2013)